 CMC, vol.24, no.1, pp.15-42, 2011

Transient Analysis of Elastic Wave Propagation in Multilayered Structures

Yi-Hsien Lin[1] **and Chien-Ching Ma**[1,2]

Abstract: In this article, explicit transient solutions for one-dimensional wave propagation behavior in multi-layered structures are presented. One of the objectives of this study is to develop an effective analytical method for constructing solutions in multilayered media. Numerical calculations are performed by three methods: the generalized ray method, numerical Laplace inversion method (Durbin's formula), and finite element method (FEM). The analytical result of the generalized ray solution for multilayered structures is composed of a matrix-form Bromwich expansion in the transform domain. Every term represents a group of waves, which are transmitted or reflected through the interface. The matrix representation of the solution can be used to calculate the transient response, without tracing the ray path manually. Numerical inversion of the Laplace transform by Durbin's formula is also used to construct transient responses. This numerical Laplace inversion technique has the advantage of calculating long-time transient responses for complicated multilayered structures. FEM results agree well with calculations obtained by the generalized ray method and numerical Laplace inversion.

Keywords: Multilayered structure; Transient wave; Laplace transform; Generalized ray; Durbin; FEM

1 Introduction

Wave propagation in multilayered media has long been an interesting subject due to its significance in a large number of applications in aerospace, electronic engineering, mechanical engineering, oceanography, and earthquake engineering. For example, coated-layer materials are very important in electronic engineering, where the prevention of delamination is desirable. Many studies in earthquake engineer-

[1] Department of Mechanical Engineering, National Taiwan University, Taipei, Taiwan 10617, R.O.C.

[2] Corresponding author. Tel.: +886-2-23659996; fax:+ 886-2-23631755. E-mail address: ccma@ntu.edu.tw (C. C. Ma)

ing focus on calculating the response of a multilayered medium subject to a sudden disturbance, located either on the surface or inside the medium.

The transient response induced by a dynamic load applied to the surface of a uniform half space was studied by Lamb (1904) using integral transform technique followed by the analytical evaluation of the inversion integrals. The theory and analysis of elastic waves in a stratified medium were studied in some detail in books by Ewing et al. (1957) and Brekhovskikh (1980). A transfer matrix formalism to determine the unknown coefficients from continuity conditions at interfaces of multilayered media was introduced by Thomson (1950) and improved by Haskell (1953). In earth geophysics and earthquake engineering, this matrix method was widely used to determine the dispersion relation of surface waves in a layered half-space case.

Generalized ray theory was developed in 1939, when Cagniard studied transient waves in two homogeneous half spaces in contact. In this monumental work, he showed that by going through a sequence of contour deformations and changes of integration variables, it is possible to find the inverse Laplace transforms of the expressions for each ray. A review of this theory is given by Pao and Gajewski (1977). Pekeris et al. (1965) proposed a transient wave solution for one layer overlaying the half space. The propagation of transient waves was represented by a series, with each term indicating a wave propagating through the medium. The series expansion required evaluation of a 4×4 determinant for a plate and a 6×6 determinant for a two-layered medium. Spencer (1960) used the generalized ray method to investigate the surface response of a stratified half space to radiation from a localized source. This method related an infinite series of the generalized ray integral, constructed in the Laplace transform domain, by collecting the source function, reflection and transmission coefficients, receiver function, and phase function. Ma and Huang (1996) derived the transfer relation as a general representation of the responses between each layer, instead of the displacement-traction vector, to determine the transient wave propagating in a multilayered medium. Theoretical, numerical, and experimental results for transient responses of a layered medium subject to in-plane loads were presented by Ma and Lee (2000). The dynamic response of a layered medium subject to anti-plane loads was investigated by Ma et al. (2001).

In addition to the analytical treatment, two different computational approaches exist: one based on the numerical inversion of Laplace transforms and the other on the finite element method (FEM). Idesman (2011) applied the two-stage time-integration procedure to one dimensional and two dimensional wave propagation and structural dynamics problems. Sladek et al. (2006) used the Laplace transform technique and the meshless local Petrov-Galerkin method to analyze the linear

transient coupled thermoelastic problem. Narayanan and Beskos (1982) systematically proposed eight algorithms for the numerical inversion of Laplace transforms and compared them against each other with respect to their accuracy and computational efficiency. They found that the most accurate algorithm was the method proposed by Durbin (1974), although it required more computational time. Manolis and Beskos (1981) compared the algorithms proposed by Durbin (1974) and Papoulis (1957) for the numerical Laplace inversion. They found that Durbin's algorithm was more time consuming than Papoulis' but that the accuracy was very high, even for long-time calculations. More details regarding Durbin's method and its applications to beam dynamic responses are presented by Manolis, and Beskos (1980).

Finite element methods (FEMs) offer purely numerical computations for analyzing elastodynamic problems. For example, the three-dimensional finite element method has been used to perform dynamic analysis of laminated plates under impact loads (Lee et al., 1984; Sun and Chen, 1985). In the 1960s, the rapid development of finite element methods coupled with large-scale digital computers led to the domination of such computational methods in studies of the mechanics of solids and structures, but research into analytical methods (i.e., the transfer matrix, Fourier transform, Laplace transform) has been revived in recent years due to their accuracy.

Many analytical solutions for transient wave propagation in multilayered media appear in the literature for 1-D, 2-D, and 3-D (Ma and Lee, 2006) problems. For the one-dimensional problem of plane wave propagation in the direction normal to the layering medium, Sun et al. (1968a, 1968b) present continuum theory instead of "effective modulus theory" for determining dispersion relation. Black et al. (1960) propose a chracteristics method for wave propagation in a two-layered medium. Lundergan and Drumheller (1971) numerically simulated the response in a multilayered system with varying thickness, and their results were in excellent agreement with experimental results. Harmonic waves in composites with isotropic layers were studied by Stern et al. (1971) and Hegemier and Nayfeh (1973). Transient plane waves propagating in a periodically layered elastic medium were examined by Ting and Mukunoki (1979, 1980) and Tang and Ting (1985). Recently, Chen et al. (2004) developed an analytical solution, based on Floquet's theory, for the problem of plate impact in layered heterogeneous material systems, and the agreement between analytical results and experimental data was very good.

However, all of the numerical calculations presented in these papers are limited to the case of a layered half space, or to fewer layers and early-time responses. In this article, transient responses of a multilayered structure subject to a uniformly distributed load on the surface are investigated using analytical methods. Interface

and boundary conditions are applied to obtain a system of equations for determining the global field vector, which is a stack of the field vectors in each layer. By rearranging the coefficient matrix in a special form, consisting of the diagonal, lower triangle and upper triangle parts, and extracting the diagonal part from it, the matrix Bromwich expansion is applied to obtain global phase-related reflections and transmissions of the waves in every layer. This approach automatically lends itself to ray interpretation. The closed-form solution in terms of rays, which includes all transient waves propagating through the multilayered structure, is obtained. In comparison to the generalized ray theory used in the literature, the proposed solution methodology does not require analysis of the generalized ray paths in advance. When one attempts to take into account all of the waves that are multiply reflected, the problem of wave degenerate events increases significantly as the number of reflections increases. The solution provided in this study eliminates the degeneration problems that occur in generalized ray theory and can easily be used to calculate long-time transient responses for multilayered structures, efficiently and accurately. Taking accuracy and computing time into consideration, Durbin's method for numerical inversion is used to perform long-time calculations for complicated multilayered structures. The technique presented in this study, combining a multilayered matrix-form solution and numerical Laplace inversion, will play an important role in computation for more complicated problems.

2 Formulation of a Multilayered Medium

Consider an initially undisturbed, stratified medium consisting of n layers, as shown in Fig. 1. Each layer is assumed to be elastic, homogeneous, isotropic, and perfectly bonded. The thickness of each layer is different. The stratified medium is subject to uniform loads, applied to the top surface at $t = 0$. The quantities related to the ith layer are denoted by a superscript (i), and n stratified layers contain n+2 media, including an upper and lower half space. In other words, (0) implies the upper half-space, and (n+1) implies the lower half-space.

2.1 Governing equation

We will consider plane wave propagation in the x direction, in which the only nonvanishing component of the displacement is in the x direction, and the 1-D longitudinal wave equation can be expressed as follows:

$$\frac{\partial^2 u}{\partial x^2} = S_L^2 \frac{\partial^2 u}{\partial t^2}, \tag{1}$$

where $u(x,t)$ is the longitudinal displacement and S_L is the slowness of the longi-

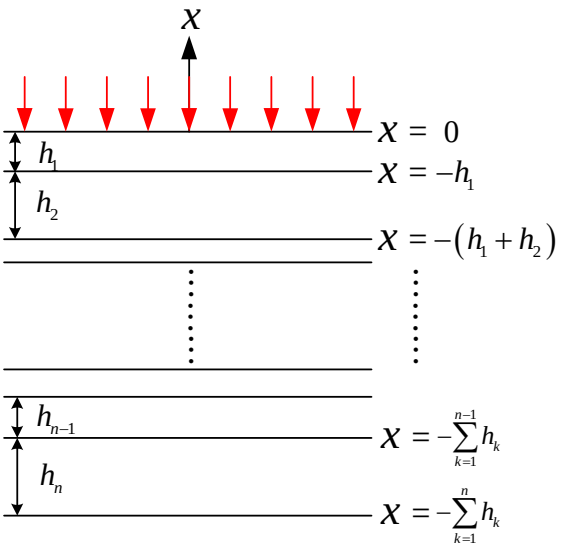

Figure 1: Configuration and coordinate system of an n-layered medium subjected to uniform loadings.

tudinal wave given by

$$S_L = 1/C_L = \sqrt{\rho/(\lambda+2\mu)},$$

in which C_L, ρ, λ, and μ are the longitudinal wave velocity, mass density, Lamé constant and shear modulus, respectively. The boundary conditions on the top and bottom layers of the multilayered medium can be written as

$$\sigma_x^{(1)}(0,t) = -\sigma_0 \cdot H(t), \tag{2}$$

$$\sigma_x^{(n)}\left(-\sum_{k=1}^{n} h_k, t\right) = 0. \tag{3}$$

The displacement and traction continuity conditions at the ith layered interface, and between two adjacent layers, are expressed as follows:

$$u^{(i)}\left(-\sum_{k=1}^{i} h_k, t\right) = u^{(i+1)}\left(-\sum_{k=1}^{i} h_k, t\right) \text{ for } i = 1,2,3,...,n-1, \tag{4}$$

$$\sigma_x^{(i)}\left(-\sum_{k=1}^{i} h_k, t\right) = \sigma_x^{(i+1)}\left(-\sum_{k=1}^{i} h_k, t\right) \text{ for } i = 1,2,3,...,n-1, \tag{5}$$

where the superscripts i in parentheses indicate the field quantities in the ith layer. For instance, $\cdot^{(i)}$and $\cdot^{(i+1)}$ denote the displacement or stress fields in the ith layer and the (i+1)th layer, respectively. The boundary value problem and continuity conditions described above are solved by applying the Laplace transform over time t with transform parameter p. The transform pair of the Laplace transformation of a function $f(x,t)$ is given by

$$\hat{f}(x;p) = \int_0^{\infty} f(x,t)\, e^{-pt} dt, \tag{6}$$

$$f(x,t) = \frac{1}{2\pi i} \int_{c-i\infty}^{c+i\infty} \hat{f}(x;p)\, e^{pt} dp. \tag{7}$$

By applying the Laplace transform, the general solution of the displacement field can be obtained from the governing equation (1),

$$\hat{u}(x;p) = u_-(p) e^{+pS_L x} + u_+(p) e^{-pS_L x}, \tag{8}$$

and the stress field follows Hooke's law,

$$\hat{\sigma}_x(x;p) = \rho C_L p u_-(p) e^{+pS_L x} - \rho C_L p u_+(p) e^{-pS_L x}. \tag{9}$$

Hence, we can rewrite these field quantities in transform domain as the displacement-traction matrix

$$\begin{bmatrix} \hat{u}(x;p) \\ \hat{\sigma}_x(x;p) \end{bmatrix} = \begin{bmatrix} M_{11}(x;p) & M_{12}(x;p) \\ M_{21}(x;p) & M_{22}(x;p) \end{bmatrix} \begin{bmatrix} u_-(p) \\ u_+(p) \end{bmatrix}, \tag{10}$$

where

$$M_{11}(x;p) = e^{+pS_L x}, \tag{11}$$

$$M_{12}(x;p) = e^{-pS_L x}, \tag{12}$$

$$M_{21}(x;p) = \rho C_L p e^{+pS_L x}, \tag{13}$$

$$M_{22}(x;p) = -\rho C_L p e^{-pS_L x}, \tag{14}$$

are phase-related receiver elements. In order to avoid complicated mathematical

expressions, the boundary and interface conditions can be represented as follows:

$$
\begin{bmatrix}
M_{21}^{(1)}(0) & M_{22}^{(1)}(0) & 0 & 0 \\
M_{11}^{(1)}(-h_1) & M_{12}^{(1)}(-h_1) & -M_{11}^{(2)}(-h_1) & -M_{12}^{(2)}(-h_1) \\
M_{21}^{(1)}(-h_1) & M_{22}^{(1)}(-h_1) & -M_{21}^{(2)}(-h_1) & -M_{22}^{(2)}(-h_1) \\
\vdots & \vdots & \ddots & \ddots \\
\vdots & \vdots & \ddots & \ddots \\
0 & \cdots & M_{11}^{(n-1)}\left(-\sum_{k=1}^{n-1} h_k\right) & M_{12}^{(n-1)}\left(-\sum_{k=1}^{n-1} h_k\right) \\
0 & \cdots & M_{21}^{(n-1)}\left(-\sum_{k=1}^{n-1} h_k\right) & M_{22}^{(n-1)}\left(-\sum_{k=1}^{n-1} h_k\right) \\
0 & \cdots & \cdots & \cdots
\end{bmatrix}
$$

$$
\begin{bmatrix}
0 & \cdots & \cdots & 0 \\
0 & \cdots & \cdots & 0 \\
\vdots & \cdots & \cdots & \vdots \\
\ddots & & & \vdots \\
\ddots & & & \vdots \\
0 & 0 & -M_{11}^{(n)}\left(-\sum_{k=1}^{n-1} h_k\right) & -M_{12}^{(n)}\left(-\sum_{k=1}^{n-1} h_k\right) \\
0 & 0 & -M_{21}^{(n)}\left(-\sum_{k=1}^{n-1} h_k\right) & -M_{22}^{(n)}\left(-\sum_{k=1}^{n-1} h_k\right) \\
\cdots & 0 & M_{21}^{(n)}\left(-\sum_{k=1}^{n} h_k\right) & M_{22}^{(n)}\left(-\sum_{k=1}^{n} h_k\right)
\end{bmatrix}
$$

$$
\cdot
\begin{bmatrix}
u_-^{(1)} \\ u_+^{(1)} \\ u_-^{(2)} \\ u_+^{(2)} \\ \vdots \\ \vdots \\ u_-^{(n)} \\ u_+^{(n)}
\end{bmatrix}
=
\begin{bmatrix}
-\frac{\sigma_0}{p} \\ 0 \\ 0 \\ \vdots \\ \vdots \\ \vdots \\ 0 \\ 0
\end{bmatrix}
\tag{15}
$$

In compact notation, the previous equation is written as

$$
\mathbf{M}\mathbf{c} = \hat{\mathbf{t}}, \tag{16}
$$

where

$$\mathbf{c} = \left(u_-^{(1)} \quad u_+^{(1)} \quad u_-^{(2)} \quad u_+^{(2)} \quad \cdots \quad u_-^{(n)} \quad u_+^{(n)}\right)^T, \tag{17}$$

and

$$\hat{\mathbf{t}} = \left(-\frac{\sigma_0}{p} \quad 0 \quad \cdots \quad \cdots \quad 0\right)^T, \tag{18}$$

and the coefficient matrix $\mathbf{M}$ is a $2n \times 2n$ matrix given by

$$\mathbf{M} = \mathbf{D} + \mathbf{L} + \mathbf{U} = \begin{bmatrix} \mathbf{D_0} & \mathbf{U_0} & & & & & \\ \mathbf{L_1} & \mathbf{D_1} & \mathbf{U_1} & & & \mathbf{0} & \\ & \mathbf{L_2} & \mathbf{D_2} & \ddots & & & \\ & & & \ddots & & & \\ & & & \ddots & \mathbf{D_{n-2}} & \mathbf{U_{n-2}} & \\ & \mathbf{0} & & & \mathbf{L_{n-1}} & \mathbf{D_{n-1}} & \mathbf{U_{n-1}} \\ & & & & & \mathbf{L_n} & \mathbf{D_n} \end{bmatrix}. \tag{19}$$

In Eq. (19), the components of diagonal matrix $\mathbf{D}$ are given by

$$\mathbf{D_0} = M_{21}^{(1)}(0), \tag{20}$$

$$\mathbf{D_i} = \begin{bmatrix} M_{12}^{(i)}(-\sum_{k=1}^{i} h_k) & -M_{11}^{(i+1)}(-\sum_{k=1}^{i} h_k) \\ M_{22}^{(i)}(-\sum_{k=1}^{i} h_k) & -M_{21}^{(i+1)}(-\sum_{k=1}^{i} h_k) \end{bmatrix} \text{ for } i = 1,2,3,...,n-1, \tag{21}$$

$$\mathbf{D_n} = M_{22}^{(n)}(-\sum_{k=1}^{n} h_k). \tag{22}$$

Note that the diagonal block matrix $\mathbf{D}$ is a nonsingular matrix. The nonzero block elements of upper triangular matrix $\mathbf{U}$ are expressed by

$$\mathbf{U_0} = \begin{bmatrix} M_{22}^{(1)}(0) & 0 \end{bmatrix}, \tag{23}$$

$$\mathbf{U}_i = \begin{bmatrix} -M_{12}^{(i+1)}(-\sum_{k=1}^{i} h_k) & 0 \\ -M_{22}^{(i+1)}(-\sum_{k=1}^{i} h_k) & 0 \end{bmatrix}, \text{ for } i = 1,2,3,...,n-1, \tag{24}$$

$$\mathbf{U}_{n-1} = \begin{bmatrix} -M_{12}^{(n)}(-\sum_{k=1}^{n-1} h_k) \\ -M_{22}^{(n)}(-\sum_{k=1}^{n-1} h_k) \end{bmatrix}, \tag{25}$$

and the nonzero block elements of lower triangular matrix $\mathbf{L}$ are

$$\mathbf{L_1} = \begin{bmatrix} M_{11}^{(1)}(-h_1) \\ M_{21}^{(1)}(-h_1) \end{bmatrix}, \tag{26}$$

$$\mathbf{L}_i = \begin{bmatrix} 0 & M_{11}^{(i)}(-\sum_{k=1}^{i} h_k) \\ 0 & M_{21}^{(i)}(-\sum_{k=1}^{i} h_k) \end{bmatrix} \text{ for } i = 2,3,...,n-1, \tag{27}$$

$$\mathbf{L}_n = \begin{bmatrix} 0 & M_{21}^{(n)}(-\sum_{k=1}^{n} h_k) \end{bmatrix}. \tag{28}$$

Eq. (16) can be solved directly by

$$\mathbf{c} = \mathbf{M}^{-1}\hat{\mathbf{t}}. \tag{29}$$

Once the global field vector $\mathbf{c}$ is obtained, the response functions in each layer can be determined. In Eq. (19), the coefficient matrix $\mathbf{M}$ can be written in an alternative form by extracting block-diagonal matrix $\mathbf{D}$ out of the expression as (Lee and Ma, 2000)

$$\mathbf{M} = \mathbf{D}\,(\mathbf{I} - \mathbf{R}), \tag{30}$$

where the matrix $\mathbf{R}$ is given by

$$\mathbf{R} = -\mathbf{D}^{-1}\,(\mathbf{L} + \mathbf{U}), \tag{31}$$

or alternatively,

$$\mathbf{R} = \begin{bmatrix} 0 & -\mathbf{D}_0^{-1}\mathbf{U}_0 & & & & & \\ -\mathbf{D}_1^{-1}\mathbf{L}_1 & \mathbf{0}_{2\times 2} & -\mathbf{D}_1^{-1}\mathbf{U}_1 & & & \mathbf{0} & \\ & -\mathbf{D}_2^{-1}\mathbf{L}_2 & \mathbf{0}_{2\times 2} & \ddots & & & \\ & & \ddots & \ddots & \ddots & & \\ & & & \ddots & \mathbf{0}_{2\times 2} & -\mathbf{D}_{n-2}^{-1}\mathbf{U}_{n-2} & \\ & \mathbf{0} & & & -\mathbf{D}_{n-1}^{-1}\mathbf{L}_{n-1} & \mathbf{0}_{2\times 2} & -\mathbf{D}_{n-1}^{-1}\mathbf{U}_{n-1} \\ & & & & & -\mathbf{D}_n^{-1}\mathbf{L}_n & 0 \end{bmatrix} \tag{32}$$

It can be shown that the elements of **R** shown in Eq. (32) are related to the phase-related reflection and transmission coefficients. First, the general waves propagating from the upper medium (i) to the lower medium (i+1) are considered. With the application of continuity conditions at the interface, the phase-related reflection coefficient $R_{i/i+1}$ at the interface between medium (i) and medium (i+1) is expressed as follows:

$$R_{i/i+1} = r_{i/i+1} e^{-2pS_L^{(i)} \sum_{k=1}^{i} h_k}, \quad r_{i/i+1} = \frac{\rho^{(i)} C_L^{(i)} - \rho^{(i+1)} C_L^{(i+1)}}{\rho^{(i)} C_L^{(i)} + \rho^{(i+1)} C_L^{(i+1)}}. \tag{33}$$

The phase-related transmission coefficient $T_{i/i+1}$ is

$$T_{i/i+1} = t_{i/i+1} e^{-p\left(S_L^{(i)} - S_L^{(i+1)}\right) \sum_{k=1}^{i} h_k}, \quad t_{i/i+1} = \frac{2\rho^{(i+1)} C_L^{(i+1)}}{\rho^{(i)} C_L^{(i)} + \rho^{(i+1)} C_L^{(i+1)}}. \tag{34}$$

Note that $r_{i/i+1}$ and $t_{i/i+1}$ are the reflection and transmission coefficients for plane waves, respectively. Next, consider the incident waves traveling upward from the lower medium (i+1) to the upper medium (i). Similarly, the phase-related reflected coefficient $R_{i+1/i}$ is

$$R_{i+1/i} = r_{i+1/i} e^{+2pS_L^{(i+1)} \sum_{k=1}^{i} h_k}, \quad r_{i+1/i} = \frac{\rho^{(i+1)} C_L^{(i+1)} - \rho^{(i)} C_L^{(i)}}{\rho^{(i)} C_L^{(i)} + \rho^{(i+1)} C_L^{(i+1)}}, \tag{35}$$

and the phase-related transmission coefficient $T_{i+1/i}$ is

$$T_{i+1/i} = t_{i+1/i} e^{-p\left(S_L^{(i)} - S_L^{(i+1)}\right) \sum_{k=1}^{i} h_k}, \quad t_{i+1/i} = \frac{2\rho^{(i)} C_L^{(i)}}{\rho^{(i)} C_L^{(i)} + \rho^{(i+1)} C_L^{(i+1)}}. \tag{36}$$

The global phase-related reflection and transmission matrix **R**, given in Eq. (32), can be rewritten in terms of the local reflection and transmission coefficients as follows:

$$\mathbf{R} = \begin{bmatrix}
0 & R_{1/0} & & & & & & & & \\
R_{1/2} & 0 & 0 & T_{1/2} & & & & & \mathbf{0} & \\
T_{2/1} & 0 & 0 & R_{2/1} & & & & & & \\
 & & R_{2/3} & 0 & 0 & T_{2/3} & & & & \\
 & & T_{3/2} & 0 & 0 & R_{3/2} & & & & \\
 & & & & \ddots & \ddots & \ddots & \ddots & & \\
 & & & & \ddots & \ddots & \ddots & \ddots & & \\
 & & & & & & R_{n-1/n} & 0 & 0 & T_{n-1/n} \\
 & \mathbf{0} & & & & & T_{n/n-1} & 0 & 0 & R_{n/n-1} \\
 & & & & & & 0 & 0 & R_{n/n+1} & 0
\end{bmatrix}. \tag{37}$$

From Eq. (29) and Eq. (30), the global field vector $\mathbf{c}$ is then obtained by

$$\mathbf{c} = (\mathbf{I} - \mathbf{R})^{-1}\,\mathbf{s}, \tag{38}$$

where the source vector $\mathbf{s}$ is given by

$$\mathbf{s} = \mathbf{D}^{-1}\hat{\mathbf{t}}, \tag{39}$$

or in a component form,

$$\mathbf{s} = \left(-\mathbf{D}_0^{-1}\frac{\sigma_0}{p} \quad 0 \quad \cdots \quad 0 \quad 0\right)^T. \tag{40}$$

Furthermore, we can relate the response vector $\mathbf{b}$ to the global field vector $\mathbf{c}$ with a phase-related receiver matrix $\mathbf{R}_{\mathbf{cv}}$ by arranging the response functions in each layer into this response vector:

$$\mathbf{b}(x;p) = \mathbf{R}_{\mathbf{cv}}(x;p)\,(\mathbf{I} - \mathbf{R})^{-1}\,\mathbf{s}, \tag{41}$$

where the phase-related receiver matrix is given by

$$\mathbf{R}_{\mathbf{cv}}(x;p) = \begin{bmatrix} M_{11}^{(1)}(x;p) & M_{12}^{(1)}(x;p) & & & & & & \\ M_{21}^{(1)}(x;p) & M_{22}^{(1)}(x;p) & & & & & & \\ & & M_{11}^{(2)}(x;p) & M_{12}^{(2)}(x;p) & & & & \\ & & M_{21}^{(2)}(x;p) & M_{22}^{(2)}(x;p) & & & & \\ & & & & \ddots & & & \\ & & & & & & M_{11}^{(n)}(x;p) & M_{12}^{(n)}(x;p) \\ & & & & & & M_{21}^{(n)}(x;p) & M_{22}^{(n)}(x;p) \end{bmatrix}. \tag{42}$$

It is noted that $\mathbf{b}$ is the response vector of multilayered structures in transform domain. With the transformed solution at hand, the inverse transform is performed to obtain the transient solution in time domain.

However, for the Laplace inversion, we will use two different methods to obtain the time domain response, the generalized ray method and numerical inverse method. In the generalized ray method, the transient response of the layered medium is decomposed into an infinite number of rays, which arrive at the receiver along a ray path in sequence. For the numerical inversion method, the well-known numerical method (Durbin's method), a combination of finite Fourier sine and cosine transforms, will be used in this study.

2.2 Generalized ray solution

As an alternative way to solve Eq. (41), generalized ray theory was used to calculate the transient response of the multilayered structure by expanding the inversion matrix of $(\mathbf{I}-\mathbf{R})$ in a Neumann series:

$$(\mathbf{I}-\mathbf{R})^{-1}=\sum_{i=0}^{\infty}\mathbf{R}^{i}. \tag{43}$$

Substitute Eq. (43) into Eq. (38), and the global field vector $\mathbf{c}$ is obtained as

$$\mathbf{c}=\sum_{i=0}^{\infty}\mathbf{R}^{i}\mathbf{s}. \tag{44}$$

Thus, the response vector $\mathbf{b}$ in Eq. (41) can be rewritten as

$$\mathbf{b}(x)=\mathbf{R}_{\mathbf{cv}}\sum_{i=0}^{\infty}\mathbf{R}^{i}\mathbf{s}, \tag{45}$$

or in the component form as follows:

$$b_l=\sum_{i=0}^{\infty}\sum_{r=1}^{2n}\sum_{q=1}^{2n}(R_{cv})_{lr}\left(R^{i}\right)_{rq}s_q, \tag{46}$$

where the subscript l varies from 1 to $2n$ and represents the displacement and stress components in each layer (i.e., b_1, b_2, and b_3 represent the displacement field in the 1st layer, the stress field in the 1st layer, and the displacement field in the 2nd layer, respectively). The symbol $\left(R^{i}\right)_{rq}$ in Eq. (46) denotes the (r,q) entry of power matrix $\mathbf{R}^{i}$, and the number i in the summation sign is not unlimited but is a fixed number in transient response for a finite time, meaning that we have to know how many rays are reflected by or transmitted through the interface during the observation time at a receiver.

Using a simple, two-layered structure as an illustrative example, the response vector $\mathbf{b}$ in Eq. (45) is a 4×1 vector, and the phase-related receiver matrix $\mathbf{R}_{\mathbf{cv}}$ is a 4×4 matrix. Moreover, the global phase-related reflection and transmission matrix $\mathbf{R}$ is a 4×4 matrix, and source vector $\mathbf{s}$ is a 4×1 vector. The matrix-form formulation Eq. (45) can be worked out, and the stress field in transform domain can be expressed as follows:

$$\begin{aligned}\hat{\sigma}_x^{(1)}(x,p)=&\sum_{i=0}^{\infty}(-\sigma_0)\cdot\left(r_{1/2}\right)^{m_1}\left(r_{1/0}\right)^{m_2}\left(r_{2/1}\right)^{m_3}\left(r_{2/3}\right)^{m_4}\left(t_{1/2}\right)^{m_5}\left(t_{2/1}\right)^{m_6}\\&\cdot\frac{1}{p}e^{\left(-S_L^{(1)}h_1(m_1+m_2+m_5+rem(i,2))-S_L^{(2)}h_2(m_3+m_4+m_6)+(-1)^{i}S_L^{(1)}x\right)\cdot p}.\end{aligned} \tag{47}$$

Furthermore, the Laplace inversion of the function involving p in Eq. (47) is

$$\mathscr{L}^{-1}\left\{\frac{e^{-pa}}{p}\right\} = H(t-a). \tag{48}$$

The transient solution for the normal stress in time domain is explicitly expressed as

$$\sigma_x^{(1)}(x,t) = \sum_{i=0}^{\infty}(-\sigma_0)\cdot\left(r_{1/2}\right)^{m_1}\left(r_{1/0}\right)^{m_2}\left(r_{2/1}\right)^{m_3}\left(r_{2/3}\right)^{m_4}\left(t_{1/2}\right)^{m_5}\left(t_{2/1}\right)^{m_6}$$
$$\cdot H\left(t - S_L^{(1)}h_1(m_1+m_2+m_5+rem(i,2)) - S_L^{(2)}h_2(m_3+m_4+m_6) + (-1)^i S_L^{(1)}x\right), \tag{49}$$

where $i = m_1+m_2+m_3+m_4+m_5+m_6$.

The transient stress field in the first layer of a two-layered medium is represented in Eq. (49), and $r_{i/i+1}$, $r_{i+1/i}$, $t_{i/i+1}$, and $t_{i+1/i}$ are the transmission and reflection coefficients as presented in Eqs. (33)-(36). The values $m_1 \sim m_6$ indicate a ray path containing different numbers of transmissions and reflections in each layer; for example, $m_1 \sim m_4$ represents the reflections from medium (1) to (2), medium (1) to (0), medium (2) to (1), and medium (2) to (3), respectively. The transmissions from medium (1) to (2) and medium (2) to (1) are represented by m_5 and m_6, respectively. In other words, we have to know how many transmissions and reflections are present in a ray path. If these ray paths are summed up in Eq. (49), the transient response during the observation time can be obtained. Note that there is a particularly interesting term in Eq. (49), indicated as $rem(i,2)$ to represent the remainder after i divided by 2, which is one or zero. This is a statistical result in order to construct a relationship between traveling time and the number of transmissions or reflections from the source to a receiver.

Table 1: Material constants used in this paper

	$\rho(kg/m^3)$	$C_L(m/s)$
Brass	8600	4437
Steel	7850	5878
Aluminum	2700	6197

Now consider two homogeneous, isotropic layers with the same thickness as that shown in Fig. 2. This medium consists of two different materials, 10 *cm* of brass and 10 *cm* of aluminum. The material constants for these two materials are listed

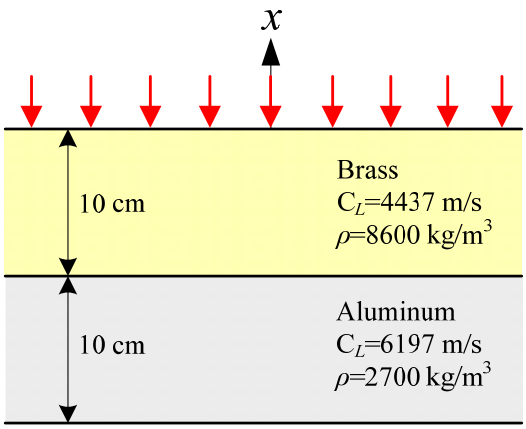

Figure 2: A uniformly distributed load applies at the top surface of a two-layered medium.

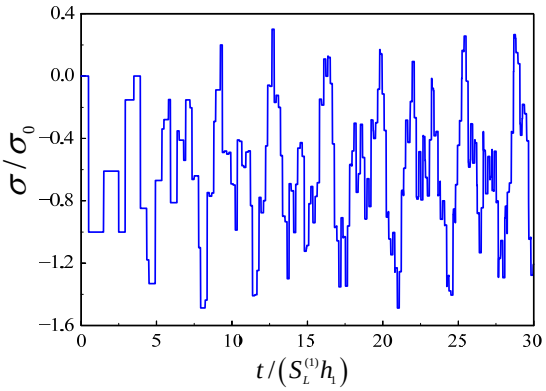

Figure 3: Transient response of stress at $x = -5cm$ in a two-layerd medium by generalized ray method.

in Table 1. A uniformly distributed load is applied at the top surface, $x = 0$, and the receiver is set at the midpoint of first layer, i.e., $x = -5cm$. In Fig. 3, the transient response, based on the generalized ray method, is presented at this position. Note that the horizontal axis is expressed as normalized time $t/S_L^{(1)}h_1$, and the vertical axis as normalized stress σ/σ_0. One can see that the source ray arrives at time $t/S_L^{(1)}h_1 = 0.5$, and the first reflecting ray from the interface arrives at time $t/S_L^{(1)}h_1 = 1.5$ (the ray path is shown in Fig. 4(a)). The third ray arrives at time $t/S_L^{(1)}h_1 = 2.5$ (shown in Fig. 4(b)). The fourth ray arrives at time $t/S_L^{(1)}h_1 = 2.932$

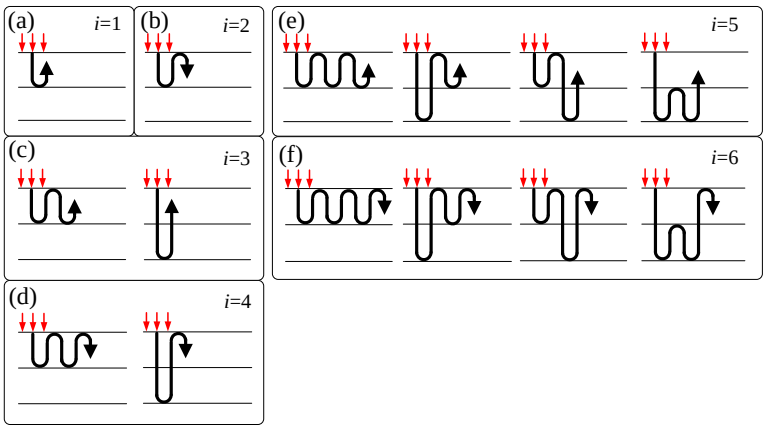

Figure 4: (a)∼(f) All possible ray paths from i= 1 to i= 6.

(shown in the right part of Fig. 4(c)).

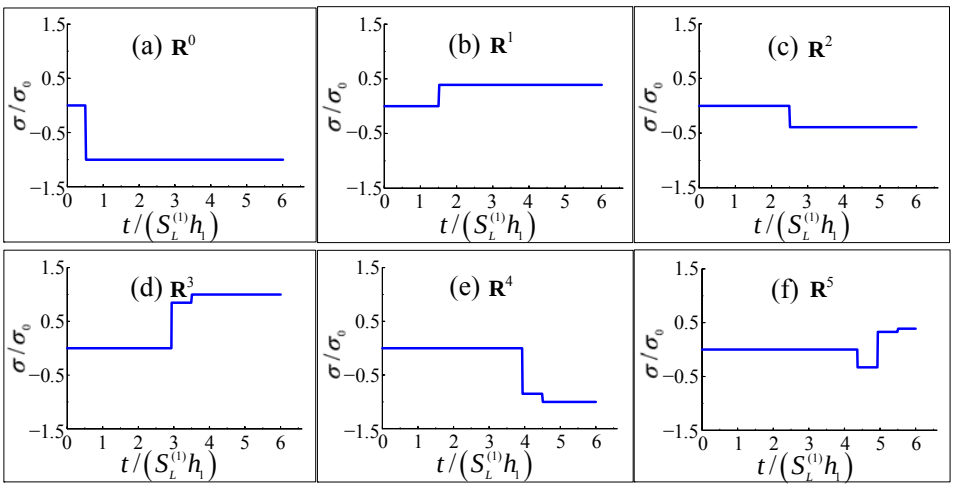

Figure 5: (a)∼(f) Decomposing the response into six groups $\mathbf{R}^0 \sim \mathbf{R}^5$ within normalized time $t/S_L^{(1)}h_1 = 6$.

To gain a better understanding of transient behavior based on the analytical methodology presented in this paper, we decomposed the response into six groups $\mathbf{R}^0 \sim \mathbf{R}^5$ within normalized time $t/S_L^{(1)}h_1 = 6$, represented in Fig. 5. These groups are sorted by the exponents of $\mathbf{R}^i$, and the exponents i imply the numbers of transmissions and

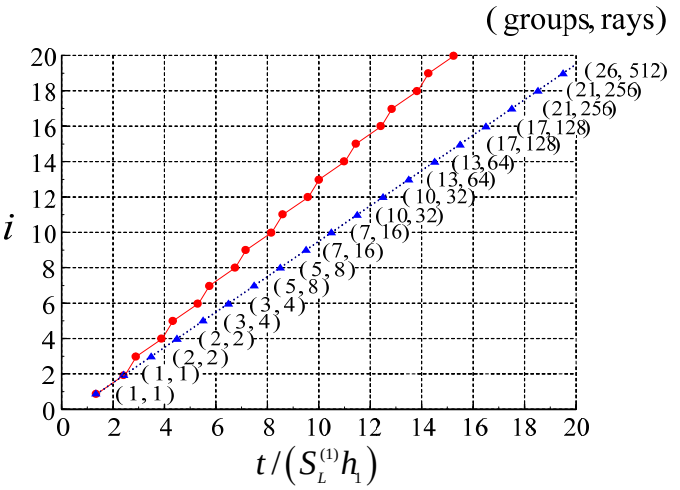

Figure 6: The number of rays and groups for multiple reflections in a two-layered medium.

reflections at interfaces or surfaces. For example, $\mathbf{R}^0$ indicates the source ray and also implies that the number of reflections or transmissions through the interfaces is zero. Similarly, $\mathbf{R}^1$ represents the wave reflected by the interface or transmitted through the interface only once. If we take the sum of $\mathbf{R}^0 \sim \mathbf{R}^5$ at the midpoint of first layer, the early-time response within $t/S_L^{(1)}h_1 = 6$ is the same as that presented in Fig. 3.

In the subsequent discussion, we sort all rays with the same number i according to travel time and set as a group those rays having the same travel time. In Fig. 6, the fastest group is represented by red solid dot, and the slowest group is represented by blue solid triangle. When $i = 1$ or 2, there is only one ray path, as indicated in Fig. 4(a) and 4(b); thus we set it into a group (or expressed as (groups, rays)=(1,1)). When $i = 3$ or 4, there are two possible ray paths from source to the receiver, as indicated in Fig. 4(c) and 4(d); however, the travel times for the two rays are different. The ray paths can be divided into two groups according to travel time, such that each group contains one ray path (or expressed as (groups, rays)=(2,2)). When $i = 5$ or 6, rays have four possible paths, seen for example in Fig. 4(e)-(f), and three groups of individual rays can be set by travel time (or expressed as (groups, rays)=(3,4)). Subsequently, in Fig. 4(e)-(f), we should note that there are two paths (i.e., the second and third ray path) with the same arrival time among four paths, and we therefore set both of them to be one group. This process is referred to as the "degeneration of rays". As the number i increases, the degeneration of

rays becomes more and more serious. For example, 512 total rays are degenerated into 26 groups when $i = 19$, and 524288 rays are degenerated into 101 groups when $i = 40$.

It is worth noting from Fig. 6 that the travel times of the fastest and slowest groups are $t/S_L^{(1)}h_1 = 5.34$ and 6.5 when $i = 6$, the travel times of the fastest and slowest groups are $t/S_L^{(1)}h_1 = 9.6$ and 12.5 when $i = 12$, and the travel times of fastest and slowest groups are $t/S_L^{(1)}h_1 = 13.86$ and 18.5 when $i = 18$. This is an important phenomenon, indicating that the time interval between the fastest group and the slowest one grows with increasing i. The figure also shows that total 32 rays are divided into 10 groups when $i = 12$, and the travel time of the fastest group is $t/S_L^{(1)}h_1 = 9.6$. When $i = 13$, however, the travel time of the fastest group is larger than 10, i.e., $t/S_L^{(1)}h_1 = 10.02$. Hence, the transient response should be evaluated with $t/S_L^{(1)}h_1 = 10$ only for $i = 0 \sim 12$ in Eq. (45) to avoid missing any possible rays. In order to understand the relationship between rays and groups, we plot the rays-groups graph in Fig. 7. This figure shows that the number of rays will increase exponentially as the number of groups gradually becomes larger. Due to this trend, the generalized ray method becomes too complex for calculation of the long-time response in complicated, multilayered media. However, the computational time can be significantly reduced if the concept of degeneration of rays is taken into account.

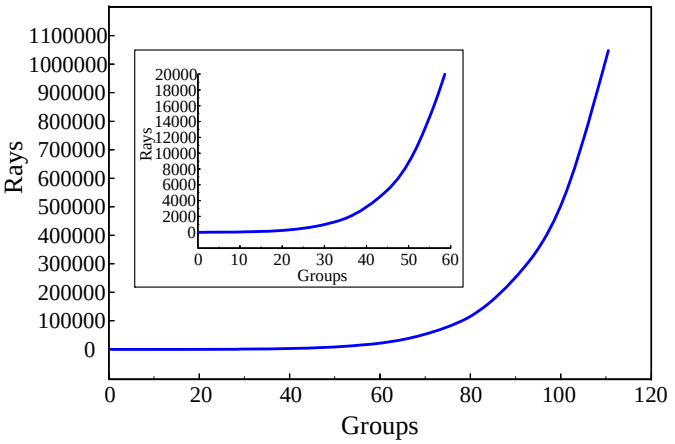

Figure 7: Relationship between rays and groups in a two-layered medium.

It is noted that different types of waves in a generalized ray can have the same expression, and this phenomenon is referred to as degeneration of waves. When we attempt to take into account all of the waves that are multiply reflected and

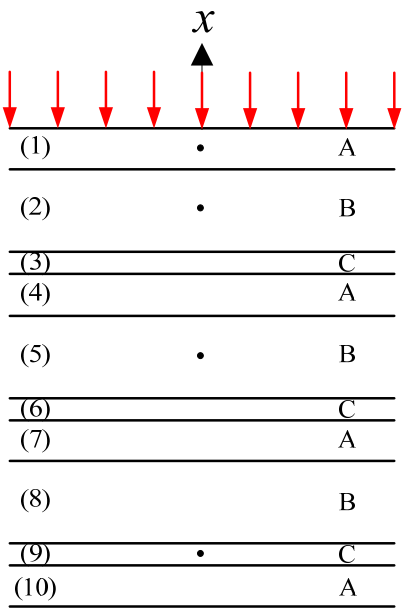

Figure 8: A 10-layered medium is composed of A, B, C materials, and the receivers are located at the midpoints of 1st, 2nd, 5th, and 9th layer.

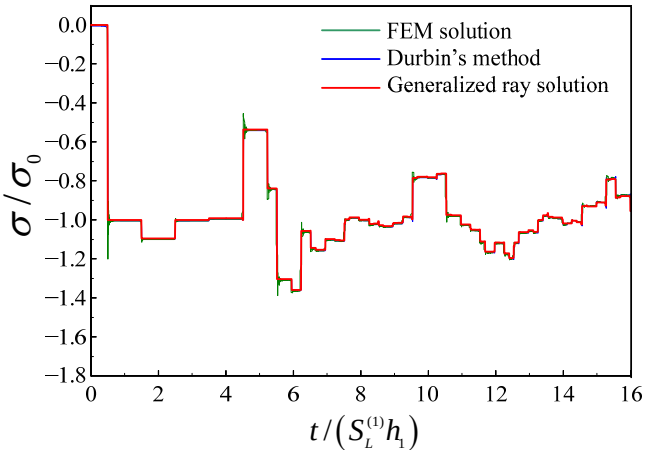

Figure 9: Transient response at the midpoint of 1st layer of a 10-layered medium obtained by generalized ray method, Durbin's inversion method and FEM.

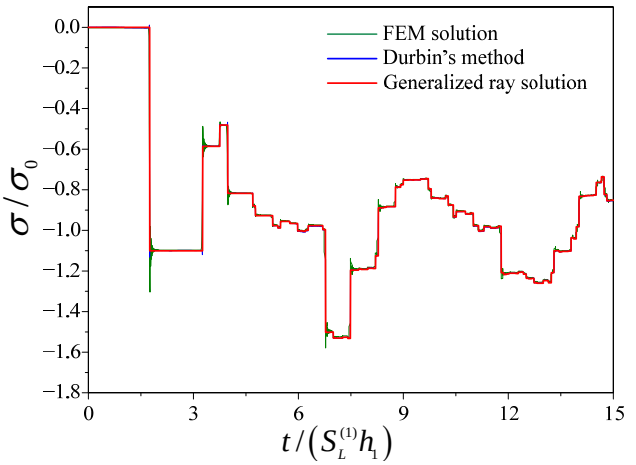

Figure 10: Transient response at the midpoint of 2nd layer of a 10-layered medium obtained by generalized ray method, Durbin's inversion method and FEM.

transmitted along the interfaces, we encounter the problem of wave degeneration immediately. Because degenerate rays are identical, only composite events have physical significance. Furthermore, the number of degenerate events increases significantly as the number of layers increases. This study introduces a better method for removing the degeneration, as otherwise the ray-tracing technique becomes extremely inefficient from a computational standpoint. The problem of degeneration can be eliminated by collecting the terms with the same coefficients in the power matrix series of the phase-related reflection and transmission matrix $\mathbf{R}$. The power matrix of $\mathbf{R}$ can be worked out in symbolic form beforehand by a program to facilitate numerical calculation.

The major advantage of the generalized ray method is that if one can evaluate all the rays passing through the receiver, the transient result is exact and accurate. Hence, it is important to describe all the possible rays propagating from the source to the receiver and to group and sort them systematically. According to the power of $\mathbf{R}^i$, the number i indicates the number of transmissions and reflections at interfaces in the layered solid, and it is very helpful for establishing the numerical program. Every term in the generalized ray solution possesses its own physical significance.

Although the presentation of summation in the generalized ray method avoids solving the boundary-value problem, it becomes impossible to handle long-time calculations. In the next section, we use a numerical Laplace inversion directly before applying series expansion to Eq. (41) and obtain the transient response in the time domain.

2.3 Numerical Laplace inversion

Transient behavior can be obtained via the Laplace transform and numerical inversion proposed by different researchers in the literature, including Durbin (1974), Papoulis (1957), Narayanan and Beskos (1982). In this paper, we use the method proposed by Durbin, which is an accurate and efficient method for numerically inverting Laplace-transformed functions, in a combination of finite Fourier sine and cosine transforms.

In Durbin's method, the inverse Laplace transformation of a function $\hat{f}(p)$ is expressed as the following series:

$$\begin{aligned} f(t) &= \frac{1}{2\pi i}\int_{c-i\infty}^{c+i\infty} \hat{f}(p)\, e^{pt} dp \\ &= \frac{2e^{\alpha t}}{T}\left\{ -\frac{1}{2} Re\left[\hat{f}(\alpha)\right] + \sum_{k=0}^{\mathrm{N}} Re\left[\hat{f}\left(\alpha + i\frac{2k\pi}{T}\right)\right] \cos\left(\frac{2k\pi t}{T}\right) \right. \\ &\quad \left. - Im\left[\hat{f}\left(\alpha + i\frac{2k\pi}{T}\right)\right] \sin\left(\frac{2k\pi t}{T}\right)\right\}. \end{aligned} \tag{50}$$

Note that the infinite series involved can only be summed up to N terms, and the transform parameter p is composed of real part α and imaginary part $\frac{2k\pi}{T}$:

$p = \alpha + ik\frac{2\pi}{T}$ for k=0, 1, 2, 3, ..., N,

in which T is the total time interval of interest, and the number of equidistant points, N, is a finite positive integer for computing $f(t)$. It is suggested that $\alpha T = 5$ to 10 can be used for good results.

We substitute the matrix-form solution, Eq. (41), into Durbin's formula, Eq. (50), and obtain the transient response in time domain by numerical calculation. The computational result and comparison of the two methods will be discussed in detail in the next section.

In the procedure for executing the traditional inversion of Laplace, branch cuts or residues are usually needed to analyze the complex plane of p. Once boundary conditions become complicated, traditional analytical Laplace inversion is too difficult to use. Moreover, Durbin's method has high accuracy for long-time calculations. The technique of numerical Laplace inversion is very important for analyzing elastodynamic problems in multilayered media and is used in this study for comparison with the results obtained by the ray method and FEM.

3 Numerical Results and Verification

ABAQUS, a widely used software package for finite element analysis, is used to analyze the elastodynamic problems in this section. An 8-node three-dimensional

element (C3D8R) with reduced integration is used to analyze transient wave behavior in a multilayered medium. Generally, reduced integration provides more accurate results and significantly reduces computational time. For Durbin's method, the computational condition $\alpha T = 10$ and summation term N=100000 are chosen to perform the numerical calculation in Eq. (50). The generalized ray solution and Durbin's Laplace inversion method for predicting the transient response in a 10-layered structure will be discussed and compared with FEM. Finally, we will analyze a 20-layered structure to investigate long-time transient responses with Durbin's inversion method and FEM.

3.1 Transient response in a 10-layered medium

First, the transient responses of a 10-layered structure subject to uniformly distributed loads with a Heaviside function are investigated in detail. This 10-layered structure shown in Fig. 8 is composed of layers A-B-C-A-B-C-A-B-C-A (A, B, C materials are A: brass, 10 cm, B: steel, 20 cm, C: aluminum, 5 cm, and material constants are listed in Table 1). The dynamic load $\sigma_0 H(t)$ is applied at the upper surface $x = 0$ (where $H(t)$ is the Heaviside step time function). The generalized ray method, Durbin's numerical inversion method, and FEM are used to construct the transient responses in the 1st, 2nd, 5th, and 9th layers, and the results are compared.

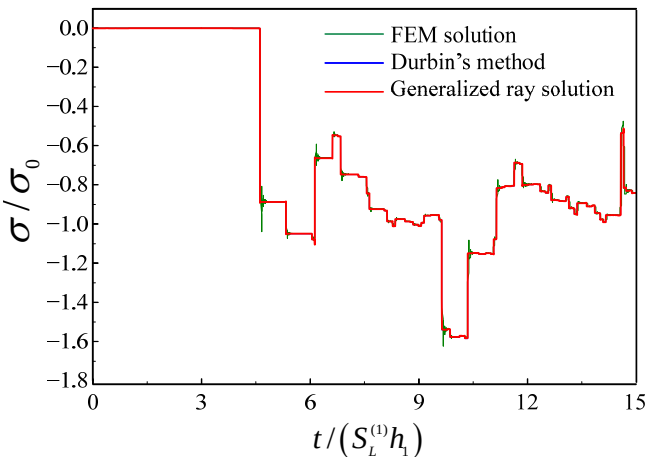

Figure 11: Transient response at the midpoint of 5th layer of a 10-layered medium obtained by generalized ray method, Durbin's inversion method and FEM.

Figs. 9-12 show the transient response of a 10-layered medium when receivers are located at the midpoints of the 1st, 2nd, 5th, and 9th layers. Wave-propagating

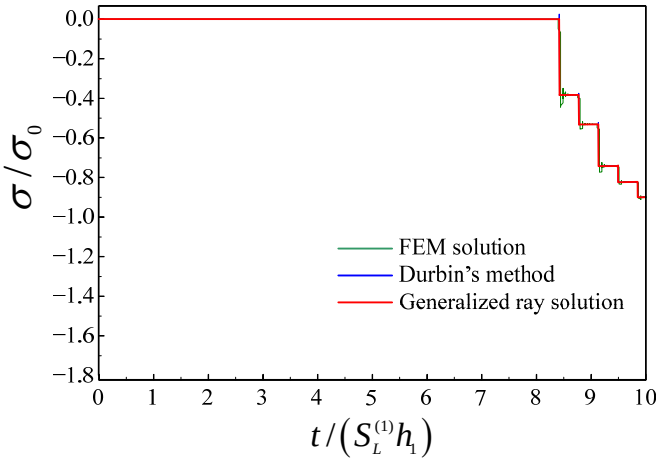

Figure 12: Transient response at the midpoint of 9th layer of a 10-layered medium obtained by generalized ray method, Durbin's inversion method and FEM.

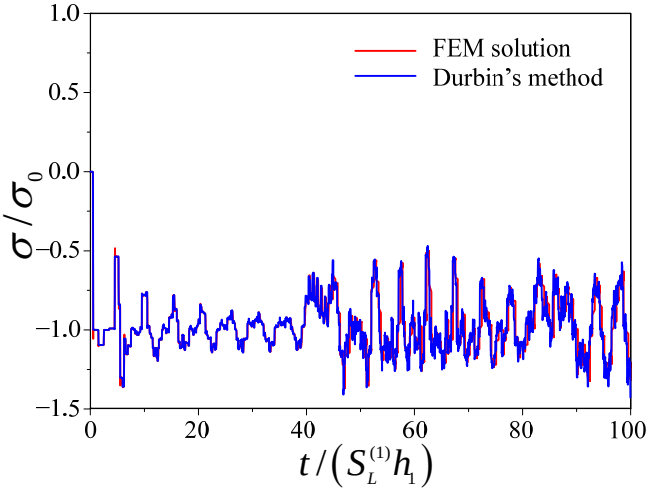

Figure 13: Long-time response at midpoint of 1st layer in a 20-layered medium obtained by Durbin's method and FEM.

behavior of the transient response for stress is evaluated by three methods: the generalized ray method (red line), Durbin's method (blue line), and FEM (green line). The results for the generalized ray method and numerical inversion method are excellently consistent. However, truncation errors known as "Gibbs phenomenon" are observed in the FEM results. This phenomenon appears only in the vicinity

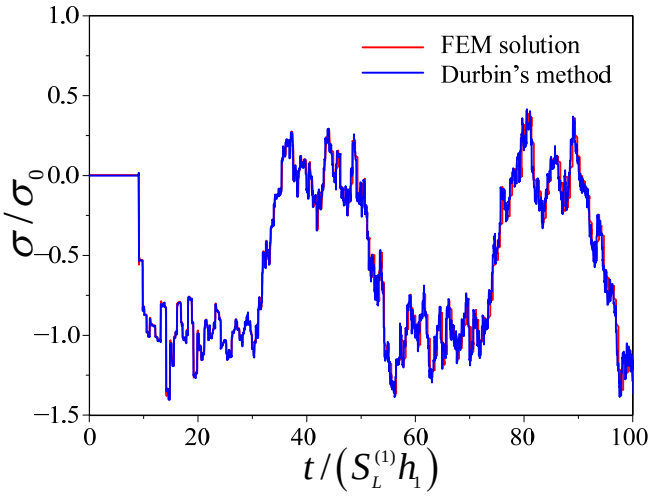

Figure 14: Long-time response at midpoint of 10th layer in a 20-layered medium obtained by Durbin's method and FEM.

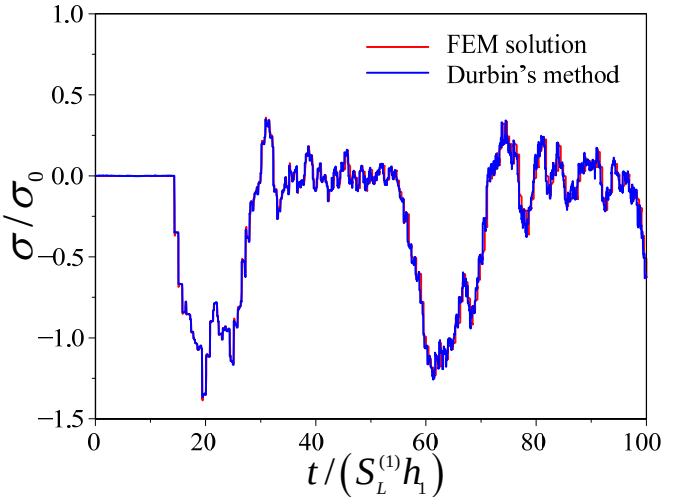

Figure 15: Long-time response at the 15-16 interface in a 20-layered medium obtained by Durbin's method and FEM.

of the discontinuity and shows up as non-physical oscillations. As shown in Figs. 9-12, the source wave arrives at the normalized times $t/S_L^{(1)}h_1 = 0.5$, 1.77, 4.57, and 8.43 for receivers located at the midpoints of the 1st , 2nd, 5th, and 9th layers,

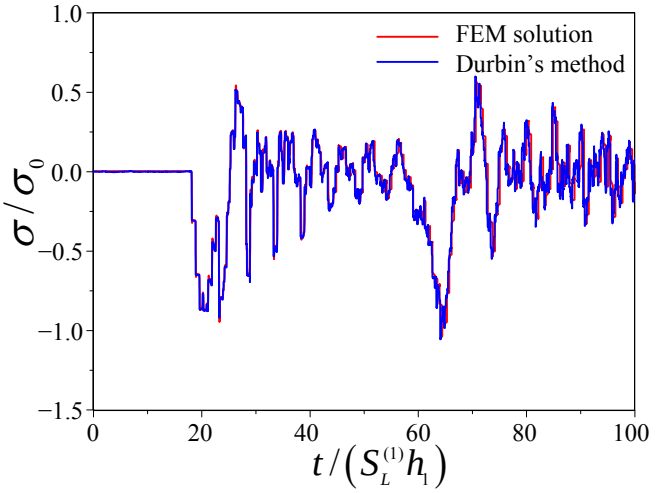

Figure 16: Long-time response at the 19-20 interface in a 20-layered medium obtained by Durbin's method and FEM.

respectively. In Fig. 9, 2252 rays are used to construct the transient response at the normalized time $t/S_L^{(1)}h_1 = 16$, and $i = 14$ is used to ensure that all ray paths are taken into account.

As shown in Fig. 9, the source wave arrives at the midpoint of the 1st layer at $t/S_L^{(1)}h_1 = 0.5$, one reflection $r_{1/2}$ arrives at $t/S_L^{(1)}h_1 = 1.5$ with magnitude $\sigma/\sigma_0 = -1.09$, and two reflections, $r_{1/2}$ and $r_{1/0}$, arrive at $t/S_L^{(1)}h_1 = 2.5$ with magnitude $\sigma/\sigma_0 = -1$. The contribution of stress waves by multiple reflections or transmissions should be considered at a later time.

The transient response in Fig. 10 is constructed from 2054 rays when $i = 14$. The source wave from the upper surface transmits directly to the receiver at the midpoint of the 2nd layer, and the magnitude of the stress jumps to $\sigma/\sigma_0 = -1.09$. The second wave, $\sigma/\sigma_0 = -0.58$, arriving at the midpoint of the 2nd layer at $t/S_L^{(1)}h_1 = 3.25$, is a reflection from the interface between the 2nd and 3rd layers, and its ray path contains one transmission, $t_{1/2}$, and one reflection, $r_{2/3}$. Transient responses at the 5th and 9th layers are expressed in Fig. 11 and Fig. 12, respectively. When $i = 14$, 1950 rays are used to obtain the response in Fig. 11, and in Fig. 12, only 12 rays and 5 groups are established when $i = 11$.

Because the number of induced waves keeps increasing with time, the generalized ray method becomes too complex to calculate the transient response in multilayered structures. For this reason, only Durbin's inversion and FEM will be used to

evaluate long-time responses in the 20-layered medium described in section 3.2.

3.2 Long-time response in a 20-layered medium

Next, a 20-layered medium containing three different materials with the sequence A-B-C-A-B-C-A-B-C-A-B-C-A-B-C-A-B-C-A-B-C-A-B and subject to uniform loads with a Heaviside function is considered. In Fig. 13, the long-time response of a 20-layered medium at position $x = -0.05m$ (the midpoint of the first layer) is presented using Durbin's numerical inversion method and FEM. The FEM solution (red line) agreed quite well with Durbin's solution (blue line) during the normalized time 40, and the number of rays induced by reflections or transmissions through the interfaces increased rapidly as the observation time gradually extended to 100. A slight difference was found between these two results for large time durations. It is indicated in Fig. 13 that the normalized stress oscillates at $\sigma/\sigma_0 = -1$ and is compressive over the whole time period.

For 10-layered and 20-layered structures, both of which are composed of three kinds of material, A, B, and C. When the receiver is set at the midpoint of the 1st layer, the transient response expressed in Fig. 9 is the same as the early-time response (within $t/S_L^{(1)}h_1 = 16$) in Fig. 13. This phenomenon indicates that waves coming from the latter ten layers had not arrived at the 1st layer.

The long-time responses at the midpoint of the 10th layer are also evaluated by Durbin's numerical inversion method and FEM, and the results are shown in Fig. 14. Both numerical results show that source waves from the upper surface arrive near the normalized time $t/S_L^{(1)}h_1 = 10$, and stress magnitude begins oscillating near $\sigma/\sigma_0 = -1$ until reflecting waves from the bottom surface arrive at the normalized time $t/S_L^{(1)}h_1 = 30$. Then, stress oscillates near $\sigma/\sigma_0 = 0$ until the reflection from the upper surface arrives at the receiver. The trend of the long-time response indicates the oscillation of wave packets between $\sigma/\sigma_0 = 0$ and $\sigma/\sigma_0 = -1$. This also implies that we can consider a 20-layered, periodic structure to be one effective layer if the receiver is set at the midpoint of the effective layer.

In Figs. 15 and 16, long-time responses for 15-16 and 19-20 interfaces are constructed by Durbin's method and FEM, respectively. The wave-propagation phenomenon in Fig. 15 is similar to that in Fig. 14. In Fig. 16, it is worth noting that the long-time response is always oscillating near $\sigma/\sigma_0 = 0$, due to the traction-free boundary condition of the bottom surface. Although the source wave is compressive, Fig. 16 shows that large tensile stresses are generated at the last interface of the multilayered medium, resulting in the delamination of the interface.

4 Conclusions

In this article, we combine the advantages of multilayered matrix-form solutions for the generalized ray method and numerical Laplace inverse to perform the computation of transient responses in multilayered structures. Long-time transient wave propagation in 10-layered and 20-layered structures are evaluated by three methods: the generalized ray method, Durbin's Laplace inverse method, and FEM. The numerical calculations of transient responses from the three methods are in good agreement. The generalized ray solution is an exact solution without numerical error, but the computational time increases rapidly for long-time responses. However, the numerical efficiency is significantly improved if the concept of degenerate waves (or wave groups) is used. A purely numerical solution by FEM using ABAQUS is capable of analyzing multilayered structures, and for long-time responses. However, numerical errors are induced during long-time calculations, and oscillations occur at abrupt changes in the response. The numerical Laplace inversion method (Durbin's method) can be considered a semi-analytic solution. Although the numerical results obtained by Durbin's inversion method do not constitute an exact solution like that of generalized ray theory, they are much more accurate than FEM and can be used for long-time calculations.

Acknowledgement: The authors gratefully acknowledge Grant NSC 98-2923-E-002-003-MY3 from the National Science Council, Republic of China, to National Taiwan University.

References

Black, M.C.; Carpenter, E.W.; Spencer, A.J.M. (1960): On the solution of one dimensional elastic wave propagation problems in stratified media by the method of characteristics. *Geophysical Prospecting,* VIII, pp. 218-230.

Brekhovskikh, L.M. (1980): *Waves in Layered Media.* Academic, New York.

Cagniard, L. (1939): *Reflexion et Refraction des ondes Seismiques Progressives*. Cauthiers-Villars, Paris; Translated into English and revised by E.A. Flinn and C.H. Dix, 1962. *Reflection and Refraction of Progressive Seismic Waves.* McGraw-Hill, New York.

Chen, X.; Chandra, N.; Rajendran, A.M. (2004): Analytical solution to the plate impact problem of layered heterogeneous material systems. *Int. J. Solids Struct.*, vol. 41, pp. 4635-4659.

Durbin, F. (1974): Numerical inversion of Laplace transforms: an efficient improvement to Dubner and Abate's method. *Computer J.*, vol. 17, pp. 371-376.

Ewing, W.M.; Jardetzky, W.S.; Press, F. (1957): *Elastic Waves in Layered Media.* McGraw-Hill, New York.

Haskell, N. (1953): The dispersion of surface waves on multilayered media. *Bull. Seism. Soc. Am.*, vol. 43, pp.17-34.

Hegemier, G.A.; Nayfeh, A.H. (1973): A continuum theory for wave propagation in laminated composites. Case 1: propagation normal to the laminates. *ASME J. Appl. Mech.*, vol. 40, pp. 503-510.

Idesman, A. (2011): Accurate time integration of linear elastodynamics problems. *CMES: Computer Modeling in Engineering & Sciences*, vol. 71, pp. 111-148.

Lamb, H. *(1904):* On the propagation of tremors over the surface of an elastic solid. Phil. Trans. Roy. Soc. London Ser. A, vol. 203, pp. 1-42.

Lee, G.S.; Ma, C.C. (2000): Transient elastic waves propagating in a multi-layered medium subjected to in-plane dynamic loadings I. theory. *Proc. R. Soc. London A*, vol. 456, pp. 1355-1374.

Lee, J.D.; Du, S.; Liebowitz, H. (1984): Three-dimensional finite element and dynamic analysis of composite laminate subjected to impact. *Comput. Struct.*, vol. 19, pp. 807-813.

Lundergan, C.D.; Drumheller, D.S. (1971): Propagation of stress waves in a laminated plate composite. *J. Appl. Phys.*, vol. 42**,** pp. 669-675.

Ma, C.C.; Lee, G.S. (2000): Transient elastic waves propagating in a multi-layered medium subjected to in-plane dynamic loadings II. Numerical calculation and experimental measurement. *Proc. R. Soc. London A*, vol. 456, pp. 1375-1396.

Ma, C.C.; Huang, K.C. (1996): Analytical transient analysis of layered composite medium subjected to dynamic inplane impact loadings. *Int. J. Solids Struct.*, vol. 33, pp. 4223-4238.

Ma, C.C.; Liu, S.W.; Lee, G.S. (2001): Dynamic response of a layered medium subjected to anti-plane loadings. *Int. J. Solids Struct.*, vol. 38, pp. 9295-9312.

Ma, C.C.; Lee, G.S. (2006): General three-dimensional analysis of transient elastic waves in a multilayered medium. *ASME J. Appl. Mech.*, vol. 73, pp. 490-504.

Manolis, G.D.; Beskos, D.E. (1981): Dynamic stress concentration studies by boundary integrals and Laplace transform. *Int. J. Numer. Meth. Eng.*, vol. 17, pp. 573-599.

Manolis, G.D.; Beskos, D.E. (1980): Thermally induced vibrations of beam structures. *Comput. Meth. Appl. Mech. Engng.*, vol. 21, pp. 337-355.

Mukunoki, I.; Ting, T.C.T. (1980): Transient wave propagation normal to the layering of a finite layered medium. *Int. J. Solids Struct.*, vol. 16, pp. 239-251.

Narayanan, G.V.; Beskos, D.E. (1982): Numerical operational methods for time-dependent linear problems. *Int. J. Numer. Meth. Eng.*, vol. 18, pp.1829-1854.

Papoulis, A. (1957): A new method of inversion of the Laplace transform. *Quart. Appl. Math.*, vol. 14, pp. 405-414.

Pao, Y.H.; Gajewski, R. (1977): *The Generalized Ray Theory and Transient Responses of Layered Elastic Solids.* in: Mason, W.P. (Ed.), Physical Acoustics, vol. 13. Academic Press, New York (Chapter 6).

Pekeris, C.L.; Alterman, Z.; Abramovici, F.; Jarosh, H. (1965): Propagation of a compressional pulse in a layered solid. *Rev. Geophys.*, vol. 3, pp. 25-47.

Sladek, J.; Sladek, V.; Zhang, Ch.; Tan, C.L. (2006): Meshless local Petrov-Galerkin method for linear coupled thermoelastic analysis. *CMES: Computer Modeling in Engineering & Sciences*, vol. 16, pp. 57-68.

Sun, C.T.; Achenbach, J.D.; Herrmann, G.. (1968a): Time-harmonic waves in a stratified medium propagating in the direction of the layering. *ASME J. Appl. Mech.*, vol. 35, pp. 408-411.

Sun, C.T.; Achenbach, J.D.; Herrmann, G.. (1968b): Continuum theory for a laminated medium. *ASME J. Appl. Mech.*, vol. 35, pp. 467-475.

Sun, C.T.; Chen, J.K. (1985): On the impact of initially stressed composite laminates. *J. Compos. Mater.* **19**, 490-504.

Spencer, T.W. (1960): The method of generalized reflection and transmission coefficients. *Geophysics*, vol. 25, pp. 625-641.

Stern, M.; Bedford, A.; Yew, C.H. (1971): Wave propagation in viscoelastic laminates. *ASME J. Appl. Mech.*, vol. 38, pp. 448-454.

Tang, Z.; Ting, T.C.T. (1985): Transient waves in a layered anisotropic elastic medium. *Proc. R. Soc. Lond.*, vol. A397, pp. 67-85.

Thomson, W.T. (1950): Transmission of elastic waves through a stratified solid medium. *J. Appl. Phys.*, vol. 21, pp. 89-93.

Ting, T.C.T.; Mukunoki, I. (1979): A theory of viscoelastic analogy for wave propagation normal to the layering of a layered medium. *ASME J. Appl. Mech.*, vol. 46, pp. 329-336.